Electronic Supplementary Information

$IrRuO_x$ catalyst supported by oxygen-vacant Ta oxide for oxygen evolution reaction and proton exchange membrane water electrolysis

Yanrong Liu [a, b, c], Meiqi Zhang [c], Cong Zhang [d], Honghua Zhang [c], Hao Wang [a, b, c] *

[a] *Beijing Key Laboratory of Ionic Liquids Clean Process, CAS Key Laboratory of Green Process and Engineering, State Key Laboratory of Multiphase Complex Systems, Institute of Process Engineering, Chinese Academy of Sciences, Beijing 100190, China.*

[b] *School of Chemical Engineering, University of Chinese Academy of Sciences, Beijing 100049, China*

[c] *Longzihu New Energy Laboratory, Zhengzhou Institute of Emerging Industrial Technology, Henan University, Zhengzhou 450000, China.*

[d] *SINOPEC Research Institute of Petroleum Processing Co., Ltd., Beijing 100083, China.*

** Corresponding author (H. Wang), Email: haowang@ipe.ac.cn*

S1. Other experimental details

S1.1 X-ray absorption characterizations

Ta L3-edge analysis was performed with Si(111)(crystal monochromators at the BLllB beamlines at the Shanghai Synchrotron Radiation Facility (SSRF) (Shanghai, China). Before the analysis at the beamline samples were pressed into thin sheets with 1 cm in diameter and sealed using Kapton tape film. The XAFS spectra were recorded at room temperature using a 4-channel Silicon Drift Detector (SDD) Bmker 5040.Ta L3-edge extended X-ray absorption fine structure (EXAFS) spectra were recorded in transmission mode. Negligible changes in the line-shape and peak position of Ta L3-edge XANES spectra were observed between two scanstaken for a specific sample. The XAFS spectra of these standard samples (For example Ta-foil and Ta_2O_5) were recorded in transmission mode. The spectra were processed and analyzed by the software codes Athena and Artemis.

S1.2 Half-cell electrochemical measurements

The OER performance was evaluated using a conventional three-electrode system connected by a PARSTAT electrochemical workstation (3000-DX, USA). To prepare the catalyst ink, 6 mg of the catalyst was ultrasonically dispersed in a mixed solution with a DI water/ethanol/Nafion (5 wt%) volume ratio of 15/35/4. The catalyst loading was controlled by the amount of ink dropped on the electrode surface. Electrochemical tests were performed in a conventional three-electrode system at room temperature in a 0.5 M H_2SO_4 electrolyte solution. A KCl-saturated Ag-AgCl electrode and a platinum sheet served as the reference and counter electrodes, respectively. All the potentials discussed below were calibrated to a reversible hydrogen electrode (RHE). To assess the OER catalytic activity of the studied samples, linear sweep voltammetry (LSV) was conducted at a scanning rate of 5 mV s^{-1} in a potential range of 1.2 – 2.0 V vs. RHE. The catalytic stability of the samples was tested by chronopotentiometry, and the current density was fixed at 10 mA cm^{-2}. Potentiostatic electrochemical impedance spectroscopy (EIS) was recorded in a frequency range of 10 kHz – 0.1 Hz at a potential

of 1.5 V vs. RHE. CV curves was recorded within the potential range of 0.624 V to 0.724 V vs. RHE, and five scanning speeds were chosen, including 20, 40, 60, 80, and 100 mV s^{-1}. The current densities taken from the middle of the curves during the charging processes were plotted as a function of the scanning rates, and the resulting slopes were C_{DL}. The catalytic stability of the samples was tested by chronopotentiometry, and the current density was fixed at 10 mA cm^{-2}.

S1.3 Single-cell PEMWE measurements

To evaluate the PEMWE performance of the studied samples, a catalyst-coated membrane (CCM) was prepared by ultrasonically spraying the anode catalyst ink and cathode catalyst ink on each side of a proton exchange membrane. To make the catalyst ink, the catalyst was dispersed into a solution containing isopropanol, deionized water, and Nafion solution (5 wt%), and the mixture was ultrasonicated over 40 min to form a uniform solution. In the catalyst ink, the dry ionomer to catalyst (I/C) ratio was 0.9 for cathode and 0.124 for anode. For all the single-cell experiments, 60wt% Pt/C (Johnson Metthey, UK) served as the cathode catalyst. The final catalyst loading on the CCM was 0.3 mg_{Ir} cm^{-2} on the anode and 0.2 mg_{Pt} cm^{-2} on the cathode as determined by an X-ray fluorescence spectrometer (HITACHI, Japan). The CCM was assembled with a carbon gas diffusion layer (GDL) on the cathode and a Ti felt porous transport layer (PTL) on the anode to finally form the membrane electrode assembly (MEA) in the electrolyzer. The single cell was maintained at 80 °C, and a flow of 80 °C water was supplied to the anode with a flow rate of 50 mL min^{-1}. The single cell was connected to a Gamry electrochemical workstation (Reference 3000, USA) equipped with a current booster (Reference 30K, USA) to record electrochemical data. Prior to testing the polarization curves, MEA was activated using 100 mA cm^{-2} for 8 h. Galvanostatic EIS was recorded in a frequency range of 1 MHz –1 Hz at a current density of 100 mA cm^{-2}. The catalytic stability of the MEAs was tested by chronopotentiometry, and the current density was fixed at 500 mA cm^{-2}.

S2. SEM images and elemental mapping for RuO_x/Ta_2O_5 and IrO_x/Ta_2O_5

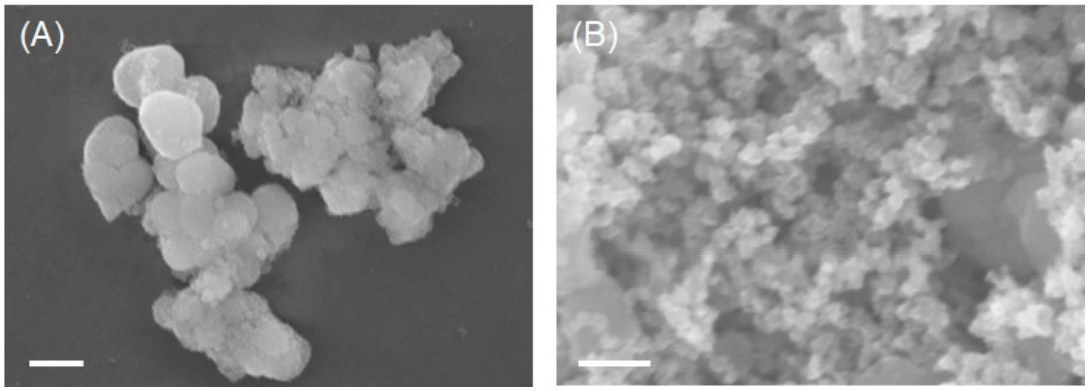

Fig. S1 SEM images of (A) Ta_2O_5 and (B) $IrRuO_x/Ta_2O_5$. Scale bar: 200 nm.

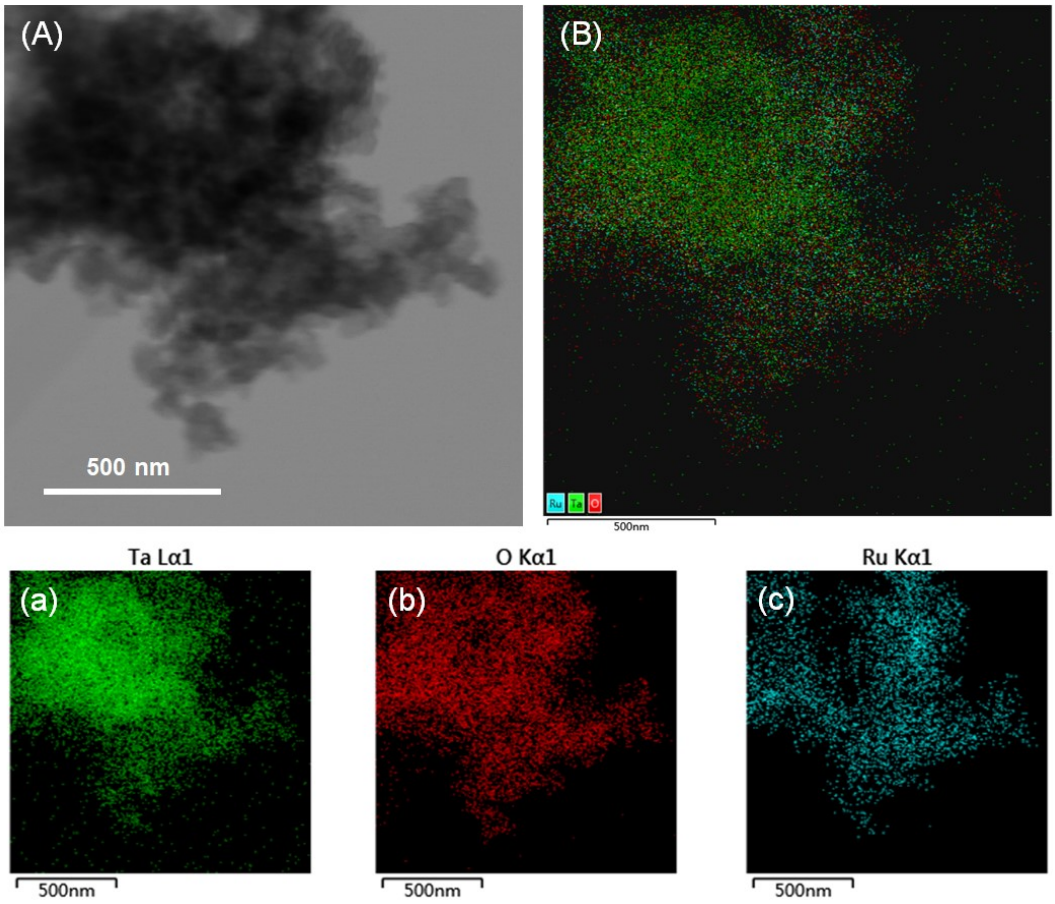

Fig. S2 (A) TEM image of the selected area to perform EDS. (B) Element mapping image with all elements overlapped. Individual element mapping of (a) Ta, (b) O, and (c) Ru for RuO_x/Ta_2O_5.

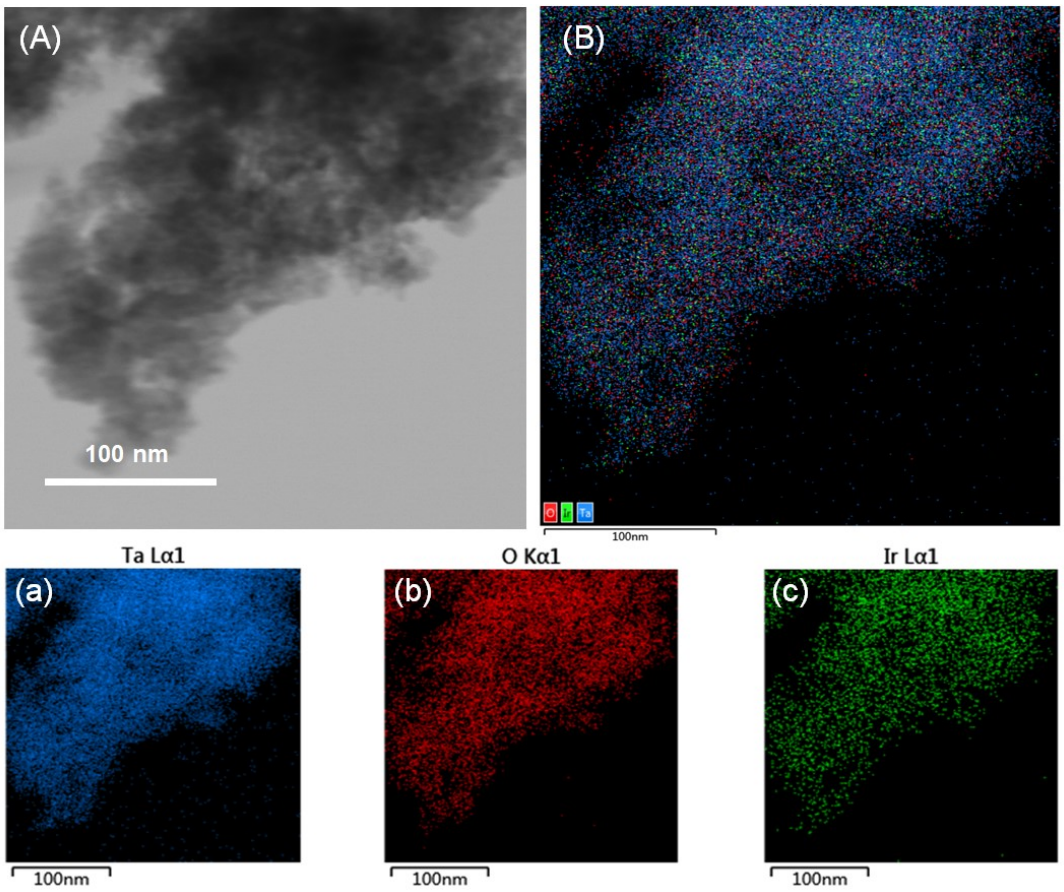

Fig. S3 (A) TEM image of the selected area to perform EDS. (B) Element mapping image with all elements overlapped. Individual element mapping of (a) Ta, (b) O, and (c) Ir for IrO_x/Ta_2O_5.

S3. Surface area and pore structures

Table S1. Summary of BET surface area and pore volume of the studied samples.

Samples	BET surface area ($m^2\ g^{-1}$)	Pore volume ($cm^3\ g^{-1}$) [a]
$IrRuO_x/Ta_2O_5$	98.18	0.043
Ta_2O_5	231.56	0.097
Ta_2O_5-C	2.92	0.001

[a] Single point adsorption total pore volume of pores less than 2.0845 nm diameter at $P/P_o = 0.205301818$

S4. XPS results

Table S2. Surface elemental contents determined by XPS and its comparison with EDS.

Elements	EDS	XPS
O	69.68	74.9
Ru	16.45	13.7
Ta	11.75	9.36
Ir	2.12	2.04

Table S3. XPS O1s spectral fitting parameters: binding energies (eV) and corresponding functional groups for the studied samples.

Samples	O 1s				
	O_L [a]	M-OH	O_V [b]	H_2O	O_{Ad} [c]
Ta_2O_5-C	530.0	--	531.1	532.1	533.2
Ta_2O_5	530.1	--	531.0	532.0	533.3
$IrRuO_x/Ta_2O_5$	529.1 (RuO_x) 530.2 (IrO_x, Ta_2O_5)	530.2	531.0	532.0	533.3
RuO_2-C	529.1	530.1	--	531.9	533.3
IrO_2-C	530.0	--	531.1	531.9	533.2

[a] O_L refers to lattice oxygen, [b] O_V refers to vacant oxygen, and [c] O_{Ad} refers to adventitious species.

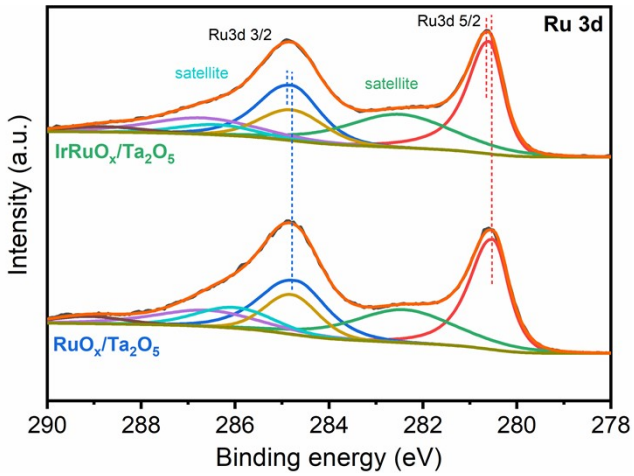

Fig. S4 XPS deconvoluted Ru 3d for $IrRuO_x/Ta_2O_5$ and RuO_x/Ta_2O_5.

S6. Double layer capacitance of the studied samples

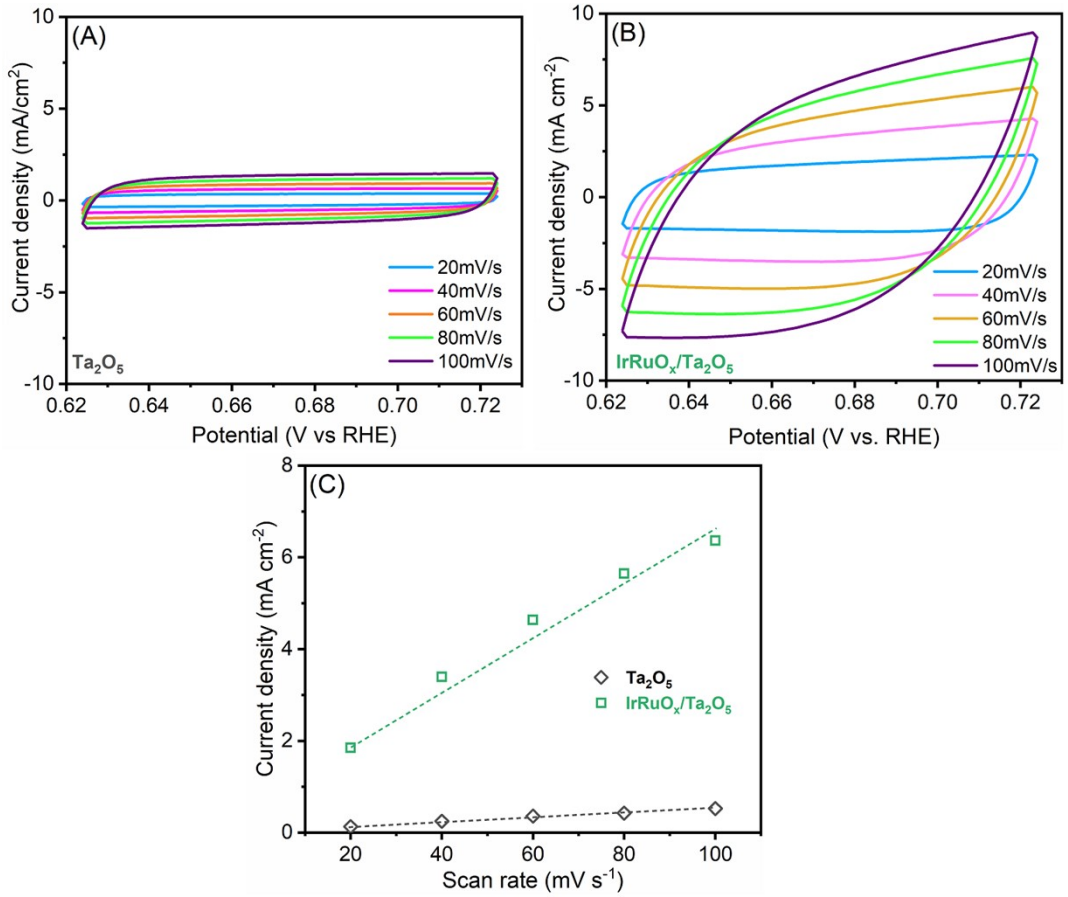

Fig. S5 CV curves at different scanning speeds for (A) Ta_2O_5 and (B) $IrRuO_x/Ta_2O_5$. (C) The double layer capacitance of the two studies samples.

S7. EXAFS fitting parameters

Table S4. EXAFS fitting parameters at the Ta L3-edge for the studied samples.

Sample	Shell	*CN*[a]	*R*(Å)[b]	σ^2(Å^2)[c]	ΔE_0(eV)[d]	*R* factor
Ta foil	Ta-Ta	8.0*	2.85±0.01	0.0047	3.3	0.0033
	Ta-Ta	6.0*	3.29±0.01	0.0061		
Ta_2O_5	Ta-O	1.2±0.1	1.82±0.01	0.0018	1.1	0.0022
	Ta-O	5.2±0.1	1.99±0.01	0.0062		
	Ta-O	1.6±0.3	3.06±0.01	0.0044	14.5	
$IrRuO_x$/ Ta_2O_5	Ta-O	1.7±0.2	1.83±0.01	0.0026	2.5	0.0044
	Ta-O	4.3±0.2	1.98±0.01	0.0066		

[a]*CN*, coordination number; [b]*R*, distance between absorber and backscatter atoms; [c]σ^2, Debye-Waller factor to account for both thermal and structural disorders; [d]ΔE_0, inner potential correction; *R* factor indicates the goodness of the fit. S_0^2 was fixed to 0.91. A reasonable range of EXAFS fitting parameters: $0.700 < S_0^2 < 1.000$; $CN > 0$; $\sigma^2 > 0$ Å^2; $|\Delta E_0| < 15$ eV; *R* factor < 0.02

S7. PEM water electrolyzer test

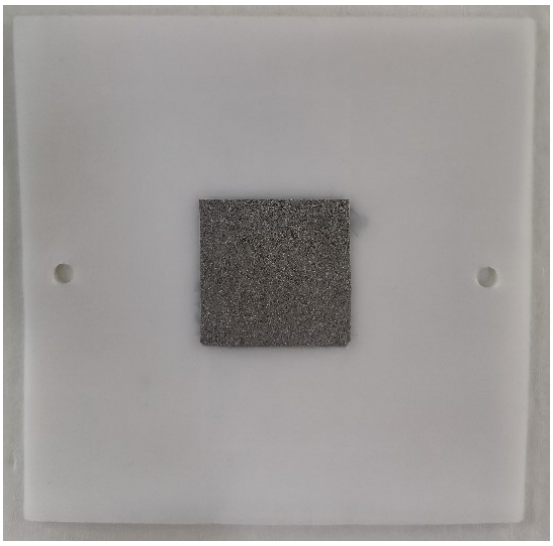

Fig. S6 A photo of an MEA configuration used in this study.

S8. OER catalytic performance comparison

Table S5. OER catalytic performance comparison between $IrRuO_x/Ta_2O_5$ and other reported Ta-supported Ir catalysts in half cells.

Catalyst	Ir loading (mg cm^{-2})	Overpotential @10mA cm^{-2} (mV)	Durability (h)	Ref.
$IrRuO_x/Ta_2O_5$	0.3	235	90 @10mA cm^{-2}	This work
$IrRuO_x/Ta_2O_5$	0.03	284	--	
IrO_2-Ta_2O_5	--	--	--	1
IrO_2-Ta_2O_5/Ti felf (350)	~0.6	270	0.5 @1.46V vs. RHE	2
$Ti/TaO_x/IrO_2$-Ta_2O_5	0.7 (total cat.)	--	--	3
IrO_2-Ta_2O_5/Ti felt(x)-PEG	0.4	~270	4 @50mA cm^{-2}	4
Ir/Ta_2O_5	--	245	200 @100mA cm^{-2}	5
IrO_2-Ta_2O_5	0.03	315	2 @10mA cm^{-2}	6
Ir/Ta_2O_5	0.03	288	3 @10mA cm^{-2}	7

References

1. W. Xu, G. M. Haarberg, S. Sunde, F. Seland, A. P. Ratvik, E. Zimmerman, T. Shimamune, J. Gustavsson and T. Åkre, *Journal of The Electrochemical Society*, 2017, **164**, F895.
2. F. Amano, Y. Furusho and Y.-M. Hwang, *ACS Applied Energy Materials*, 2020, **3**, 4531-4538.
3. Y. Liu, L. Xu, Y. Xin, F. Liu, J. Xuan, M. Guo and T. Duan, *Journal of The Electrochemical Society*, 2022, **169**, 046516.
4. F. Amano, Y. Furusho, S. Yamazoe and M. Yamamoto, *The Journal of Physical Chemistry C*, 2022, **126**, 1817-1827.
5. Y. Qiao, M. Luo, L. Cai, C.-w. Kao, J. Lan, L. Meng, Y.-R. Lu, M. Peng, C. Ma and Y. Tan, *Small*, 2023, **n/a**, 2305479.
6. H. Li, Y. Pan, L. Wu, R. He, Z. Qin, S. Luo, L. Yang and J. Zeng, *International Journal of Hydrogen Energy*, 2023, **48**, 26021-26031.
7. C. Baik, J. Cho, J. I. Cha, Y. Cho, S. S. Jang and C. Pak, *Journal of Power Sources*, 2023, **575**, 233174.